Fabrication and modeling of a continuous-flow microfluidic device for on-chip DNA amplification

George KOKKORIS, Despina C. MOSCHOU, Efie MAVRAKI, Stavros CHATZANDROULIS, and Angeliki TSEREPI*

* Corresponding author: Tel.: ++30 210 6503264; Fax: ++30 210 6511723; Email: atserepi@imel.demokritos.gr
Institute of Microelectronics, National Center for Scientific Research "Demokritos", Greece

The fabrication process and heat transfer computations for a continuous flow microfluidic device for DNA amplification by polymerase chain reaction (PCR) are described. The building blocks are thin polymeric materials aiming at a low cost and low power consumption device. The fabrication is performed by standard pattern transfer techniques (lithography and etching) used for microelectronics fabrication. The DNA sample flows in a meander shaped microchannel formed on a 100μm thick polyimide (PI) layer through three temperature regions defined by the integrated resistive heaters. The heat transfer computations are performed in a unit cell of the device. They show that, for the fabricated device, the variation of the temperature inside the channel zones where each step (denaturation, annealing, or extension) of PCR occur is less than 1.3K. This variation increases when the thickness of the PI layer increases. The computations also show that similar Silicon-based devices lead to lower temperature difference between the heaters and the DNA sample compared to the polymer-based fabricated device. However, the power consumption is estimated much greater for Silicon-based devices.

Keywords: Micro Flow, heat transfer, microfluidic device, medical device, DNA amplification, PCR

1. Introduction

Polymerase chain reaction (PCR) is used to replicate DNA and is widely used in bio-analysis such as microbial detection and medical diagnosis. PCR can create copies of specific fragments of DNA by cycling typically through three temperature steps (Crews et al., 2008): denaturation at 90–95^{o}C, annealing at 50 - 70^{o}C, and extension at 70^{o}–75^{o}C (see Fig. 1); the exact temperature of each step is defined by the pertinent protocol. Each temperature cycle can double the amount of DNA, and 20–35 cycles can produce millions of DNA copies. The development of miniaturized PCR (micro-PCR or μPCR) devices shares the motivation for μTAS (micro-Total Analysis System) (Manz et al., 1990), i.e., faster process, decreased cost for fabrication and use, portability, smaller sample size, etc. (Zhang et al., 2006). Since the early 1990s several materials (Si, glass, and recently polymers) and device designs have been utilized (Zhang et al., 2006). Even if devices generally require considerable optimization for the design and operation, and even if a series of theoretical works can be found in the literature (Chen et al., 2008; Hashimoto et al., 2004; Zhang et al., 2002), at the moment, the optimization still largely relies on a trial-and-error approach (Zhang and Ozdemir, 2009).

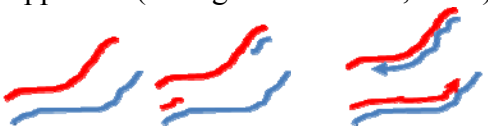

(a) (b) (c)

Figure 1. Schematic of a) denaturation, b) annealing, and c) extension of DNA.

By the exploitation of powerful commercial codes, computer aided design can replace the trial and error approach (Cao et al., 2011). Towards this aim, this work deals with both the fabrication and modeling of a continuous flow, fixed loop (Kopp et al, 1998), microfluidic device with integrated heaters for DNA amplification by PCR; the DNA sample

flows in a meander shaped microchannel through three temperature regions defined by the heaters. As PCR kinetics studies have shown that the critical parameter for an efficient process is the control of the temperature (Zhang and Ozdemir, 2009), the objective is the DNA sample temperature uniformity at each temperature region under optimum energy consumption. Quantifying the temperature uniformity, an acceptable variation is (Niu et al., 2006) ± 1.5K, i.e. 3K.

The fabrication of the continuous flow device for PCR, called here after μPCR device, is attempted on a *microheater-integrated thin polymeric* substrate (Kim 2006), for the first time to our knowledge (Giordano et al. 2001). 100μm-thick polyimide is used as substrate, featuring Cu layers on both sides. The advantages of the chosen substrate material, besides the low cost and commercial availability, include ease of fabrication (avoiding an extra metal deposition step), the ability to easily integrate the microheaters (avoiding cumbersome external heating) to facilitate portability, and reduce the power consumption as a result of the reduced thermal mass, without deteriorating temperature uniformity within each temperature zone. The device fabrication is performed by the pattern transfer techniques (lithography and etching) used for microelectronics fabrication. The modeling of μPCR deals with the numerical solution of the continuity, Navier-Stokes, and heat conduction and convection equations by the finite element method. The computations are performed for a unit cell of the device, i.e. for one thermal cycle and are used to demonstrate temperature uniformity within each thermal region and reduced power consumption for the chosen substrate.

2. The device and its fabrication

The fabricated μPCR device was formed on a thin flexible polymeric substrate using printed circuit board (PCB)-based technology. The selected substrate material was Pyralux™, a double-sided Copper-clad (Cu-clad) polyimide (PI). The thickness of PI is 100μm and the thickness of Cu is 18μm on both sides. On the top side, the microfluidic part of the device was formed, consisting of a 150μm wide and 30μm deep meander shaped microchannel. Via this channel the DNA sample will flow successively through each thermal region (denaturation at 368K → annealing at 333K → extension at 350K), completing 25 subsequent thermal cycles (Fig. 2), thus resulting in the multiplication of DNA by a factor of 2^{25}.

Each thermal region is defined by an individual Cu resistive microheater, integrated on the bottom layer of the substrate. The three resistive heaters (Fig. 3) are all meander shaped (100μm wide), in order to obtain the maximum length, thus the maximum resistance, possible.

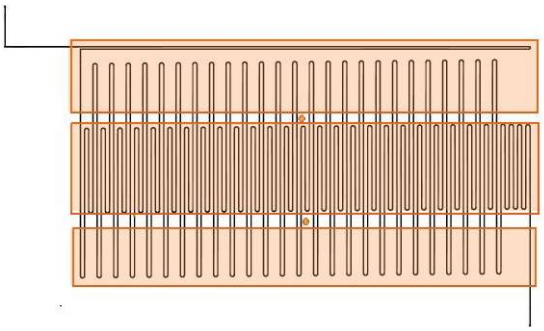

Figure 2. Top view of the chip showing the meander shaped microchannel and the three thermal regions defined by the microheaters integrated on the bottom side.

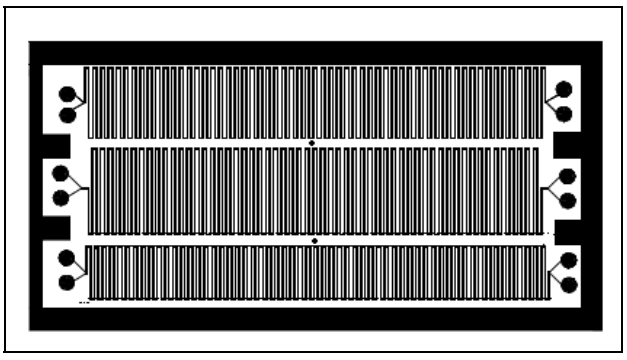

Figure 3. Lithographic mask of the three microheaters formed on the bottom Cu layer.

A visualization of the followed fabrication steps can be seen in Fig. 4. The microchannels are defined by a standard photolithography

procedure on the top Cu side. After a wet etching of the patterned top Cu layer, the channels are etched in the PI by means of plasma etching, utilizing the previously patterned Cu as a mask. The resistive heaters are formed on the bottom Cu layer also by standard photolithography and wet Cu etching procedures. That is the reason that we chose the specific double-sided Cu-clad substrate; in order to utilize the Cu layer on the top side as an etch mask and on the bottom side to integrate resistive heaters. Finally, we proceed to laminate the top side with a poly (dimethyl) siloxane (PDMS) layer adhered on polyethylene (PE), so as to seal the micro-channels (Fig. 5). The final chip size is about 7x4cm^2.

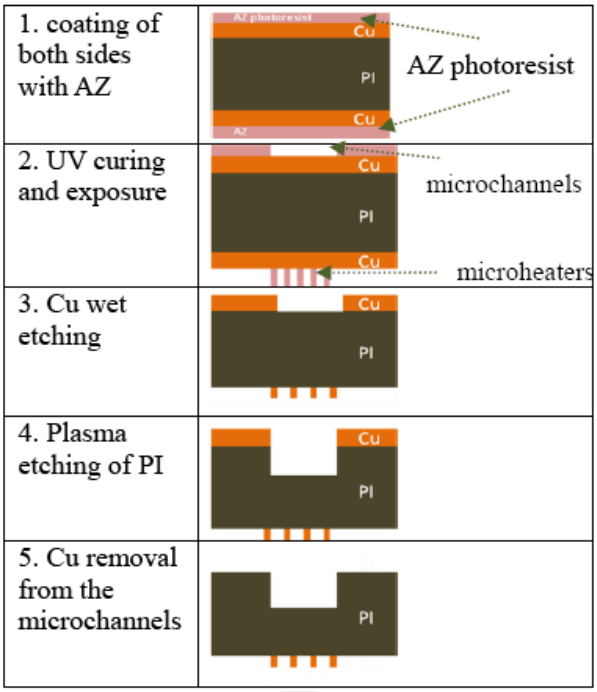

Figure 4. Process flow for the fabrication of the μPCR device with integrated heaters.

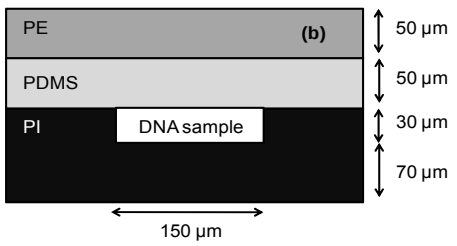

Figure 5. Cross section of the microchannel.

3. The model for heat transfer in the μPCR device

The problem of heat transfer is solved for one thermal cycle of the DNA sample, i.e. in a unit cell of the whole μPCR device. A top down view of the unit cell is shown in Fig. 6. The three meander shaped heaters, attached to the bottom of the cell, are also shown. Four channel zones are defined. At the first zone the channel is above the first heater. The second and fourth zones are above the second heater, and the third is above the third heater.

The temperature, T, is calculated at steady state by solving the equations a) for heat transfer in the solid layers of the cell

$$\nabla \cdot (-k_m \nabla T) = 0\,, \tag{1}$$

and b) for heat transfer in the fluid,

$$\nabla \cdot (-k \nabla T) = -\rho C_p \mathbf{u} \cdot \nabla T \tag{2}$$

where k_m is the thermal conductivity of the solid layer m, k, ρ, and C_p is the thermal conductivity, the density, and the specific heat of the fluid. $\mathbf{u}$ is the fluid velocity which is calculated by the Navier-Stokes and continuity equations for steady state, incompressible laminar flow,

$$\rho \mathbf{u} \cdot \nabla \mathbf{u} = \rho \mathbf{g} - \nabla p + \mu \nabla^2 \mathbf{u} \tag{3}$$

$$\nabla \cdot \mathbf{u} = 0 \tag{4}$$

where μ is the dynamic viscosity of the fluid and p is the pressure.

Periodic boundary conditions are considered for Eqs. (1) and (2) at the yz boundaries as well as at the xz boundaries at the inlet and the outlet (see Fig. 6). Constant temperatures (368K, 350K, and 333K) are considered at the interfaces of the heaters with the xy bottom boundary of the cell. At all other boundaries of the cell, convection to the ambient is considered.

Concerning Eqs. (3) and (4), the fluid enters the channel with a uniform velocity of 0.001m/s. For our design, the microchannel

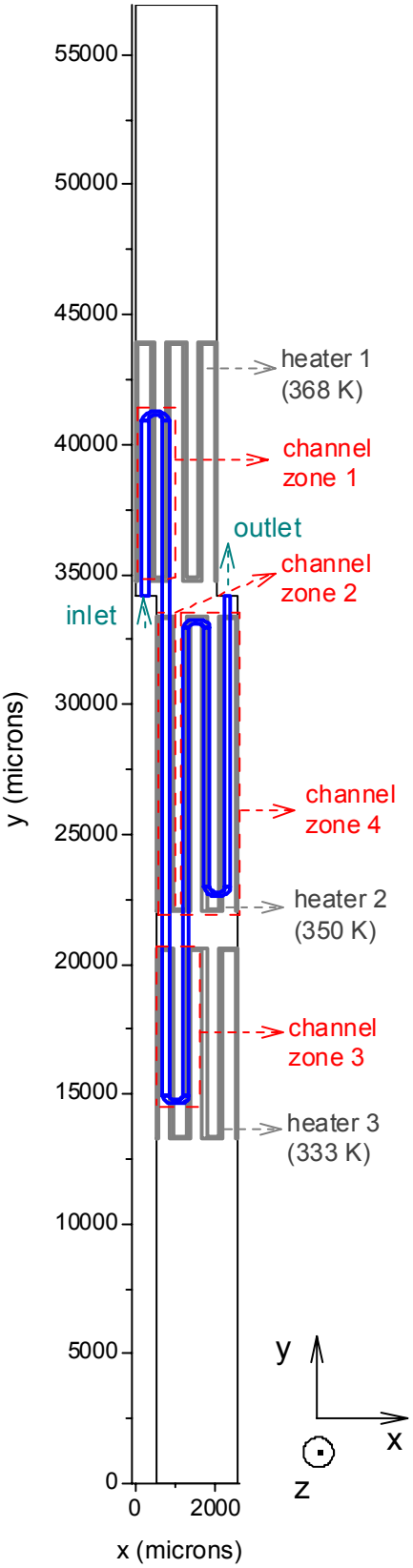

Figure 6. A top-down view of the unit cell. The three meander shaped heaters attached to the bottom of the cell are also shown. Four channel zones are defined.

length in the unit cell is about 70 mm (Fig. 6). So, with the assumed velocity, each cycle will last for about 70 sec. This is only a fraction of the time required for conventional commercial thermocyclers (about 6 min) and of the same order as other continuous-flow μPCR devices (Zhang and Ozdemir, 2009). Slip condition is considered at the channel walls, and the pressure at the outlet is set equal to zero.

The thermal conductivities of PI, PDMS, PE, and Silicon (it is used for comparison in Section 5) are (Mark, 1999; Martienssen and Warlimont, 2005) 0.1200, 0.1511, 0.445, and 149W/(m·K). The fluid properties are those of water [C_p=4200J/(kg·K), k=0.61W/(m·K), ρ=1000kg/m^3, μ=0.0036Pa·s (at 350K)].

The numerical solution is performed by the finite element method implemented by the commercial code COMSOL (www.comsol.com). The numerical mesh consists of tetrahedral elements. Linear basis functions are used for pressure and velocity components. Quadratic basis functions are used for the temperature.

The effect of the mesh density on the temperature at two points of the computation domain, i.e. on T_1 and T_2, is shown in Fig. 7. T_1 and T_2 are the temperature values at the start of zone 1 and at the end of zone 2 (see T_1 and T_2 in Fig. 8). As the number of elements increases, T_1 and T_2 tend to a saturation value. For the calculations presented in this work, 223259 (353226) elements were used for PI thickness equal to 100 (1000) μm.

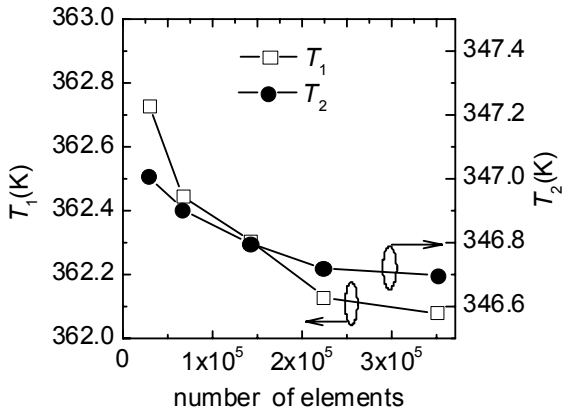

Figure 7. The effect of the number of mesh elements on the values of T_1 and T_2 (for their definition see Fig. 8).

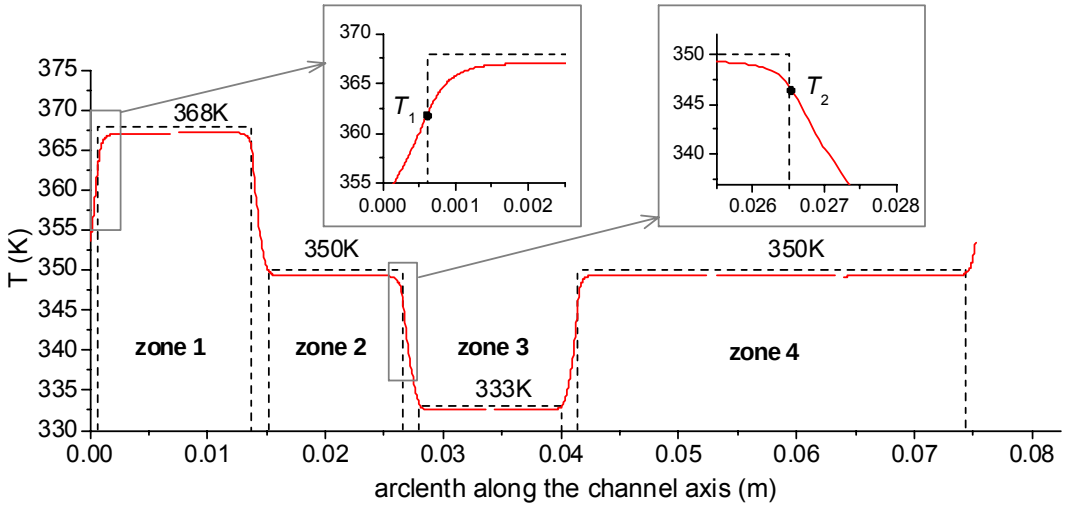

Figure 8. The fluid temperature along the arclength of the channel axis. T_1 is the temperature at the start of the zone 1 and T_2 the temperature at the end of zone 2.

4. Results and discussion

The requirement for the μPCR device is uniform fluid temperature at each one of the four zones of the channel: the temperature variation in a zone should be less than 3K (Niu et al., 2006). Additionally, the fluid temperature should be as close as possible to the set points defined by the underlying heaters.

The temperature along the arclength of the channel axis is shown in Fig. 8. The channel axis is the locus of points at the middle of the channel width and height. The temperature on a specific point on the channel is representative of the cross section of the channel at this point. High temperature uniformity is satisfied at directions normal to the channel axis. The maximum temperature variation in the fluid is calculated along the x-axis (see Fig. 6) and it is about 0.1K. This difference is due to non-alignment of the meander of the channel with the meander of the heaters. Regarding the temperature profile along the x-axis in the unit cell (fluid and solid layers), a sinusoidal oscillation is observed. This oscillation is due to the meandric shape of the heaters. The amplitude of the oscillation is below 0.2K.

As shown in Fig. 8, there is a small difference of the fluid temperature from the set point at each zone. The temperature difference is greater at the edges of each zone as demonstrated at the insets of Fig. 8.

The temperature uniformity in a channel zone i is quantified by the standard deviation, σi, of the fluid temperature along the channel axis from the mean fluid temperature, Tmean,i

$$\sigma_i = \sqrt{\frac{\sum_{j=1}^{n_i}\left[T(s_{j,i}) - T_{mean,i}\right]^2}{n_i}}\,, \quad i=1,2,3,4, \qquad (5)$$

where sj,i is the arclength of point j on the axis of the zone i. Each zone contains ni equidistant points.

The temperature difference in zone i is quantified by the average absolute difference between the temperature along the channel axis and the set point i, Tset,i, defined by the underlying heater, i.e.

$$\left|\Delta T\right|_{ave,i} = \frac{\int_{s_{1,i}}^{s_{n_i,i}} \left|T(s) - T_{set,i}\right| ds}{s_{n_i,i} - s_{1,i}}\,, \quad i=1,2,3,4. \qquad (6)$$

In Fig. 9, σ (Fig. 9a) and $|\Delta T|_{ave}$ (Fig. 9b) are shown (black bars) for each zone. The temperature differences at the start and at the end of each channel zone are the major

contributions to both σ and $|\Delta T|_{ave}$. The maximum σ is calculated for zone 1, it is 0.66K, and it implies that the temperature variation is about 1.32K in zone 1, i.e. in range of acceptable values. σ depends on the thickness of the PI layer; if the PI layer is thicker, then σ will increase. For PI thickness equal to 1000μm, σ is about 1.5K (see the white bar in Fig. 9a) and the variation is 3K, i.e. equal to the range of acceptable values. The calculations of σ for different PI thicknesses contributed to a reasonable choice for the thickness of PI layer in the fabrication process.

In order to demonstrate the differences of the proposed device with Silicon (Si) based microfluidic devices, the same calculations are performed with Si as the building material: the material of all layers is Si. The results are included in Fig. 9. Two thicknesses for the layer carrying the channel are tested as in the previous cases, i.e. 100 and 1000μm. In the low thickness case (100μm), which for Si requires a rather difficult fabrication process (the thickness of a wafer is hundreds of μm, almost 1000μm in some cases, and needs to be reduced to 100μm), σ is lower in the zones 1, 2, 4 and slightly greater in zone 3 compared to the case of the polymer-based microfluidic device. In the high thickness case (1000μm), σ for Si-based can be greater than for polymer-based device.

The Si-based devices show better performance with respect to $|\Delta T|_{ave}$ (see Fig. 9b). This is due to the high value of the thermal conductivity of Si compared to the polymeric materials (see Section 3). The results in Fig. 9b imply that in order to have the desired temperature in each zone of the polymer-based microfluidic device, i.e. 368K, 350K, 333K, the temperature of the underlying heater should be changed appropriately; generally, it should be increased as the temperature of the fluid in the channel is in most of the cases studied lower than that at the underlying heater.

Besides σ and $|\Delta T|_{ave}$, an important aspect for the design of the microfluidic device is the power required to appropriately heat the sample in each of the cases described. In order to calculate the real value for the power required, a model for the heat generation into the resistive heaters under electric potential difference is needed. In our calculations the heaters are kept at constant temperature; their temperature is not affected even if they are in contact with solid blocks with lower or higher temperature. An indication for the power consumption of the whole device can be the power required to keep the heaters at the pertinent set points. This power is calculated by summing the heat flux from the heaters to the ambient due to convection as well as the

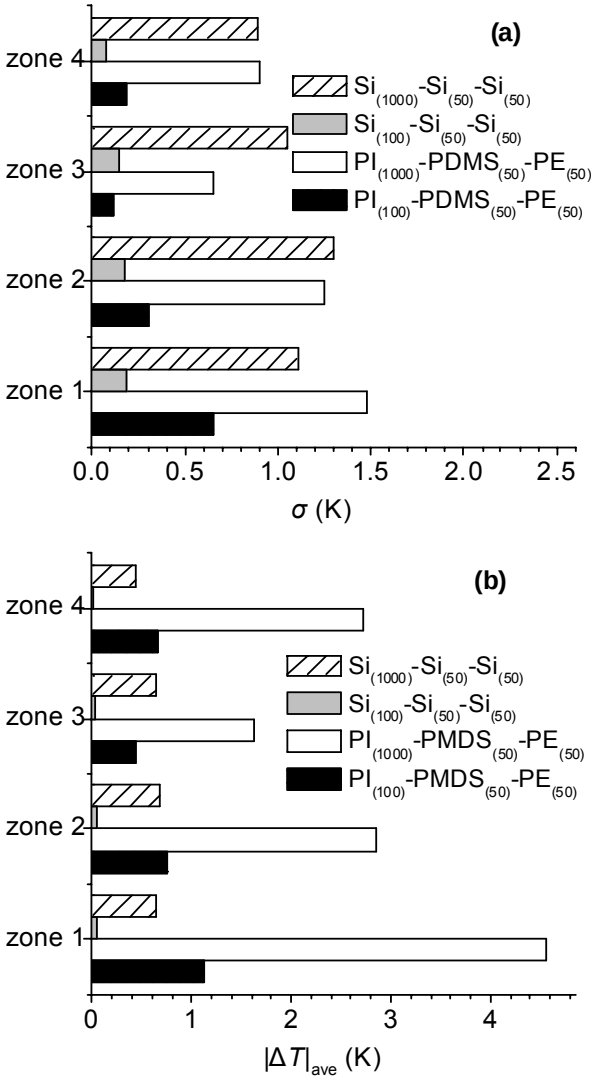

Figure 9. a) σ [see Eq. (5)] and b) $|\Delta T|_{ave}$ [see Eq. (6)] for every zone of the channel and for different thickness and material configurations. The configurations are denoted by the layer stack starting from the bottom of device. The thickness of the layer in μm is shown after the material name.

heat conduction rate to the overlying layer (PI or Si). In Fig. 10, the power required to keep the first heater at the set point is shown for all layer stacks studied. The power required for the Si-based devices is 1-2 orders of magnitude greater than for polymer-based devices.

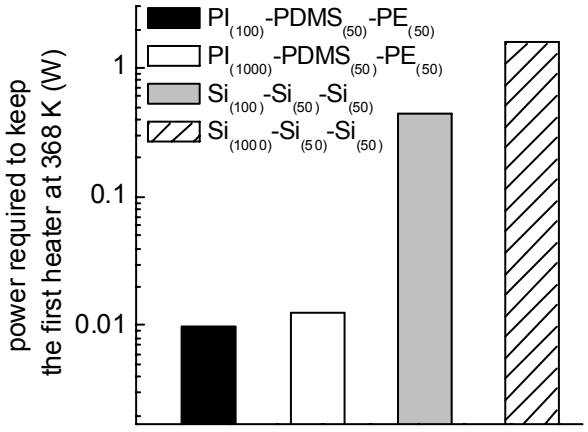

Figure 10. The power required to keep the first heater of the unit cell equal to 368 K.

5. Conclusions

The fabrication process and the concurrent modeling effort regarding a polymer-based, μPCR device with integrated heaters for DNA amplification on chip are described.

PI microchannels, through which the DNA sample flows, are formed on the top side of the chip and Cu heaters are formed on the bottom, defining the three different thermal regions required. The final fabricated chip size is about 7x4cm^2.

The calculations show that, for the chosen PI thickness (100μm), the variation of the temperature inside the channel zones, where denaturation, annealing, and extension occur, is about 1.3K. The increase of the thickness of the PI layer which is in contact with the heaters increases this variation; at a thickness of 1000μm it is about 3K.

The calculations also show that Si-based devices lead to lower temperature difference between the heaters and the DNA sample compared to the polymer-based microfluidic device. However, the power consumption is estimated much greater for Si-based devices.

Regarding the fabrication process, electrical characterization of the heaters is currently being conducted, in order to specify the required electrical currents to achieve the corresponding temperature for each thermal zone. Also, test fluids are being driven, in the temperatures of interest, through the micro-channels to verify the robustness of the sealing.

Regarding the modeling effort, the work in progress refers to the inclusion of a model for heat generation inside the resistive heaters in order to make an accurate estimation of the power required for the device operation.

Nomenclature

C_p: Specific heat [J/(kg·K)]
k: Thermal conductivity [W/(m·K)]
n: Number of points in a channel zone.
p: Pressure of the fluid (Pa)
s: Arclength of a point on the axis of a channel zone (m).
T: Temperature (K).
T_{mean}: Mean fluid temperature in a channel zone (K).
T_{set}: Set point of a channel zone defined by the underlying heater (K).
u: Fluid velocity vector (m/s).

$|\Delta T|_{ave}$: Average absolute difference between the fluid temperature along the channel axis and the set point in a channel zone (K).
μ: Dynamic viscosity of the fluid (Pa·s).
ρ: Density (kg/m^3).
σ: Standard deviation of the fluid temperature along the channel axis from the mean fluid temperature in a channel zone (K).

i: Index for a channel zone.
j: Index for a point in a channel zone.
m: Index for a solid layer of the device.

Acknowledgments

This work was co-financed by Hellenic Funds and by the European Regional

Development Fund (ERDF) under the Hellenic National Strategic Reference Framework (NSRF) 2007-2013, according to Contract no. MICRO2-45 of the Project "Microelectronic Components for Lab-on-chip molecular analysis instruments for genetic and environmental applications" within the Programme "Hellenic Technology Clusters in Microelectronics – Phase-2 Aid Measure".

References

Cao Q.Q., Kim M.-C., Klapperich C. 2011. Plastic microfluidic chip for continuous-flow polymerase chain reaction: Simulations and experiments. Biotechnol. J. 6, 177.

Chen, P.C., Nikitopoulos, D.E., Soper, S.A., Murphy, M.C., 2008. Temperature distribution effects on micro-CFPCR performance. Biomed Microdevices 10, 141-152.

Crews, N., Wittwer, C., Gale, B., 2008. Continuous-flow thermal gradient PCR. Biomed Microdevices 10, 187-195.

Giordano B.C., Ferrance J., et al. 2001. PCR in polymeric microchips: DNA amplification in less than 240 s. Analytical Biochemistry 291, 124-132.

Hashimoto, M., Chen, P.C., Mitchell, M.W., Nikitopoulos, D.E., Soper, S.A., Murphy, M.C., 2004. Rapid PCR in a continuous flow device. Lab on a Chip 4, 638-645.

Kim Y.S. 2006. Microheater-integrated single gas sensor array chip fabricated on flexible polyimide substrate. Sensors & Actuators B 114, 410-417.

Kopp M. U., de Mello A. J., Manz A. Chemical Amplification: Continuous-Flow PCR on a Chip. Science, 15 May 1998, 1046-1048.

Manz, A., Graber, N., Widmer, H.M., 1990. Miniaturized Total Chemical-Analysis Systems - a Novel Concept for Chemical Sensing. Sens. Actuator B-Chem. 1, 244-248.

Mark, J.E., 1999. Polymer Data Handbook. Oxford University Press.

Martienssen, W., Warlimont, H., 2005. Springer Handbook of Condensed Matter and Materials Data. Springer.

Niu, Z.Q., Chen, W.Y., Shao, S.Y., Jia, X.Y., Zhang, W.P., 2006. DNA amplification on a PDMS-glass hybrid microchip. J. Micromech. Microeng. 16, 425-433.

www.comsol.com.

Zhang, C.S., Xu, J.L., Ma, W.L., Zheng, W.L., 2006. PCR microfluidic devices for DNA amplification. Biotechnol Adv 24, 243-284.

Zhang, Q., Wang, W., Zhang, H., Wang, Y., 2002. Temperature analysis of continuous-flow micro-PCR based on FEA. Sens. Actuator B-Chem. 82, 75.

Zhang, Y.H., Ozdemir, P., 2009. Microfluidic DNA amplification-A review. Analytica Chimica Acta 638, 115-125.